Journal of Hazardous Materials 173 (2010) 173–180

Contents lists available at ScienceDirect

Journal of Hazardous Materials

journal homepage: www.elsevier.com/locate/jhazmat

# Preparation, characterization and thermolysis of nitrate and perchlorate salts of 2,4,6-trimethylaniline☆

Inder Pal Singh Kapoor[a], Manisha Kapoor[a], Gurdip Singh[a,*], Udai P. Singh[b], Nidhi Goel[b]

[a] Department of Chemistry, DDU Gorakhpur University, Gorakhpur 273009, India
[b] Department of Chemistry, Indian Institute of Technology, Roorkee, Roorkee 247667, India

ARTICLE INFO

*Article history:*
Received 7 July 2009
Received in revised form 13 August 2009
Accepted 14 August 2009
Available online 22 August 2009

*Keywords:*
Explosion
Ignition
Thermolysis
Nitrate
Perchlorate

ABSTRACT

Nitrate and perchlorate salts of 2,4,6-trimethylaniline have been prepared and characterized by X-ray crystallography and gravimetric analyses. Their thermal decomposition has been studied by TG, TG–DSC and ignition/explosion delays. It has been observed that proton transfer from substituted anilinium ion to nitrate and perchlorate ion regenerate amine, $HNO_3$ and $HClO_4$ in condensed phase at higher temperature, where oxidation–reduction between amine and acids leads to ignition and explosion. The kinetics of thermal decomposition was evaluated by applying model fitting as well as isoconversional methods. The values of calculated activation energy of nitrate and perchlorate salts are 77.9 and 118.2 kJ mol$^{-1}$ respectively. The possible pathways of thermolysis of these salts have also been proposed.



## 1. Introduction

Because of the presence of both the oxidizer and the fuel parts in the same molecule, nitrate and perchlorate salts finds applications in explosive, pyrotechnics and propellant formulations [1]. Nitrates are powerful oxidizing agent which decompose and ignite at elevated temperature to give oxygen as one of the major products [2,3]. The perchlorates have been reported to sublime, decompose at lower temperatures and explode readily at higher temperatures. These are generally more violent in their explosive behavior as compared to nitrate salts [4,5]. Erdey and co-workers [6,7] have investigated the thermal decomposition of various ammonium salts and results have been explained on the basis of acid–base theory.

A lot of work on the thermolysis of various energetic, transition metal complexes and ring (mono and di) substituted ammonium salts (nitrates and perchlorates) have been done [8–13] and proton transfer [14] was generally found to be the primary and the rate determining step. The number and nature of (ring) substituted groups play an important role in thermolysis of ammonium salts. As a part of our ongoing research program we report here preparation, crystal structure, characterization and thermolysis of 2,4,6-trimethylanilinium nitrate (2,4,6-TMAN) and 2,4,6-trimethylanilinium perchlorate (2,4,6-TMAP) salts.

## 2. Experimental

### 2.1. Materials

2,4,6-trimethylaniline, 70% Nitric acid, 70% Perchloric acid (Merck), Silica gel TLC grade (Rankem), Iodine (s.d.fine) and Nitron (CDH) were used as received.

### 2.2. Preparation and characterization

The salts (Caution: explosion hazards) were prepared by treating amine with corresponding acids (Cold 20% $HNO_3$, and Cold 20% $HClO_4$) directly in 1:2 molar ratio in accordance with the reaction (Scheme 1).

The salts were recrystallized from double distilled water. Their purity was checked by thin layer chromatography (TLC) using suitable solvent. Moreover, these salts were characterized by X-ray crystallography and gravimetric methods using nitron reagent. The physical parameters are shown in Table 1.

### 2.3. Crystallographic study

Single crystal of 2,4,6-TMAN and 2,4,6-TMAP were obtained by recrystallization from their aqueous solution. The X-ray data collection were performed on Brucker Kappa Apex–CCD diffractometer

☆ Part-75.

* Corresponding author. Tel.: +91 551 2200745/+91 551 2202856; fax: +91 551 234045.
*E-mail address:* gsingh4us@yahoo.com (G. Singh).

0304-3894/$ – see front matter © 2009 Elsevier B.V. All rights reserved.
doi:10.1016/j.jhazmat.2009.08.058

**Table 1**
Physical parameters, TLC, gravimetric analyses of 2,4,6-TMAN and 2,4,6-TMAP.

| Compound | Structure | Crystal | M.P. (°C) | TLC | $R_f$ | Gravimetric estimation |
|---|---|---|---|---|---|---|
| 2,4,6-TMAN | 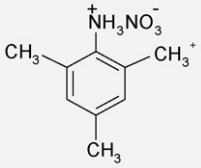 | White tiny particle | 182 | a:b:c | 0.95 | 89% |
| 2,4,6-TMAP | 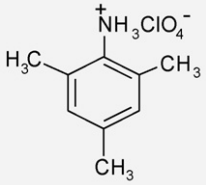 | Transparent rectangular | 204 | a:c:d | 0.71 | 92% |

Eluent: a = Dioxane, b = ethyl acetate, c = chloroform, d = water; Locating reagent: Iodine.

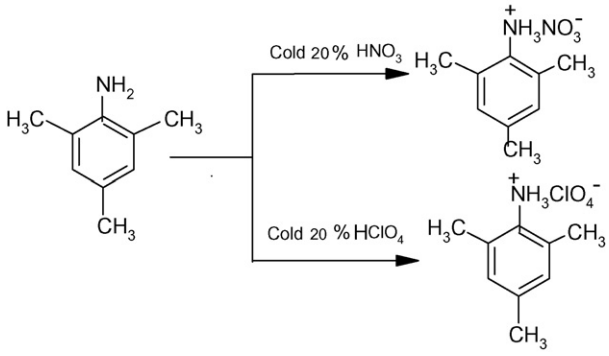


**Scheme 1.** Preparation of 2,4,6-TMAN and 2,4,6-TMAP from 2,4,6-trimethylaniline.

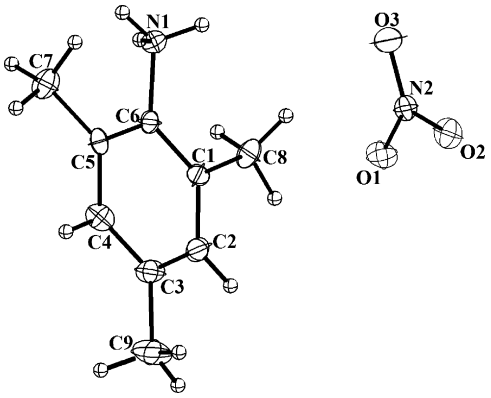


**Fig. 1.** Thermal ellipsoidal presentation for molecular structure of 2,4,6-TMAN with 30% probability factor.

**Table 2**
Crystal data and structure refinement of 2,4,6-TMAN and 2,4,6-TMAP.

| | | |
|---|---|---|
| Empirical formula | $C_9H_{14}N_2O_3$ | $C_9H_{14}ClNO_4$ |
| Formula weight | 198.22 | 235.66 |
| Temperature | 100(2) K | 100(2) K |
| Wavelength | 0.71073 Å | 0.71073 Å |
| Crystal system, space group | Monoclinic, *P*21/*n* | Triclinic *P*-1 |
| Unit cell dimensions | *a* = 10.998(3) Å | *a* = 7.207(2) Å |
| | *b* = 8.189(2) Å | *b* = 8.616(3) Å |
| | *c* = 11.770(3) Å | *c* = 9.138 Å |
| | *(* = 106.198(13) | *α* = 88.933(18)° |
| | | *(* = = 78.643(19)º |
| | | *γ* = 87.072(19)° |
| Volume | 1018.0(5) Å$^3$ | 555.6(3) Å$^3$ |
| *Z* | 4 | 2 |
| Calculated density | $1.293 \times 10^{-9}$ g cm$^{-3}$ | $1.409 \times 10^{-9}$ g cm$^{-3}$ |
| Absorption coefficient | 0.098 mm$^{-1}$ | 0.338 mm$^{-1}$ |
| *F*(0 0 0) | 424 | 248 |
| Crystal size | 0.228 × 0.217 × 0.182 mm | 0.228 × 0.217 × 0.182 mm |
| Theta range | 3.07–26.48° | 3.27–32.35° |
| Limiting indices | −13<= *h* <=13, | −10<= *h* <=10, |
| | −10<= *k* <=9, | −12<= *k* <=12, |
| | −12<= *l* <=14 | −13<= *l* <=13 |
| Max. and min. transmission | 0.940 and 0.927 | 0.982 and 0.978 |
| Refinement method | Full matrix least-square on $F^2$ | Full matrix least-square on $F^2$ |
| Data/restraints/parameters | 3843/0/140 | 3843/0/140 |
| Goodness-of-fit on $F^2$ | 1.211 | 1.211 |
| Final *R* indices [$I > 2\sigma(I)$] | *R*1 = 0.0482 w$R^2$ = 0.1512 | *R*1 = 0.0520 w$R^2$ = 0.1730 |
| *R* indices (all data) | *R*1 = 0.0654 w$R^2$ = 0.1650 | *R*1 = 0.0775 w$R^2$ = 0.1920 |
| CCDC No. | 734678 | 734679 |

**Table 3**
Bond lengths [Å] of 2,4,6-TMAN and 2,4,6-TMAP.

| 2,4,6-TMAN | | 2,4,6-TMAP | |
|---|---|---|---|
| O1–N2 | 1.2511(18) | Cl1–O1 | 1.4359(19) |
| O2–N2 | 1.2522(18 | Cl1–O2 | 1.4374(17) |
| O3–N2 | 1.2197(17) | Cl1–O3 | 1.4229(18) |
| N1–C6 | 1.4664(19) | Cl1–O4 | 1.4250(15) |
| C1–C2 | 1.393(2) | N1–C2 | 1.471(2) |
| C1–C6 | 1.388(2) | C1–C6 | 1.384(3) |
| C1–C8 | 1.496(2) | C1–C2 | 1.390(3) |
| C2–C3 | 1.374(3) | C1–C8 | 1.518(3) |
| C3–C4 | 1.389(3) | C2–C3 | 1.396(3) |
| C3–C9 | 1.509(3) | C3–C4 | 1.381(3) |
| C4–C5 | 1.389(2) | C3–C7 | 1.515(3) |
| C5–C6 | 1.387(2) | C4–C5 | 1.515(3) |
| C5–C7 | 1.497(2) | C5–C6 | 1.391(3) |
| N1–H1A | 0.8900 | C5–C9 | 1.506(3) |
| N1–H1B | 0.8900 | N1–H1A | 0.8900 |
| N1–H1C | 0.8900 | N1–H1B | 0.8900 |
| C2–H2 | 0.9300 | C7–H7B | 0.9600 |
| C4–H4 | 0.9300 | C7–H7C | 0.9600 |
| C7–H7A | 0.9600 | C8–H8A | 0.9600 |
| C7–H7B | 0.9600 | C8–H8B | 0.9600 |
| C7–H7C | 0.9600 | C8–H8C | 0.9600 |
| C8–H8A | 0.9600 | C9–H9A | 0.9600 |
| C8–H8B | 0.9600 | C9–H9B | 0.9600 |
| C8–H8C | 0.9600 | C9–H9C | 0.9600 |
| C9–H9A | 0.9600 | | |
| C9–H9B | 0.9600 | | |
| C9–H9C | 0.9600 | | |

**Table 4**
Bond Angle of 2,4,6-TMAN and 2,4,6-TMAP.

| 2,4,6-TMAN | | 2,4,6-TMAP | |
|---|---|---|---|
| O3–N2–O1 | 121.60(15) | O1–Cl1–O2 | 108.53(11) |
| O3–N2–O2 | 120.62(15) | O3–Cl1–O1 | 109.19(14) |
| O1–N2–O2 | 117.77(13) | O3–Cl1–O2 | 109.50(12) |
| C6–C1–C2 | 116.74(14) | O3–Cl1–O4 | 110.54(11) |
| C6–C1–C8 | 121.82(14) | O4–Cl1–O1 | 109.88(13) |
| C2–C1–C8 | 121.44(14) | O4–Cl1–O2 | 109.17(10) |
| C3–C2–C1 | 122.73(15) | C2–N1–H1A | 109.5 |
| C2–C3–C4 | 118.30(15) | C2–N1–H1B | 109.5 |
| C2–C3–C9 | 121.13(17) | C2–N1–H1C | 109.5 |
| C4–C3–C9 | 120.58(18) | C6–C1–C2 | 117.27(17) |
| C3–C4–C5 | 121.64(15) | C6–C1–C8 | 121.15(18) |
| C6–C5–C4 | 117.67(15) | C2–C1–C8 | 121.57(19) |
| C6–C5–C7 | 122.08(15) | C1–C2–C3 | 123.31(18) |
| C4–C5–C7 | 120.25(15) | C4–C3–C2 | 116.67(17) |
| C5–C6–C1 | 122.84(14) | C4–C3–C7 | 120.89(17) |
| C5–C6–N1 | 119.93(13) | C2–C3–C7 | 122.43(18) |
| C1–C6–N1 | 117.22(13) | C3–C4–C5 | 122.61(18) |
| C6–N1–H1A | 109.5 | C6–C5–C4 | 118.10(19) |
| C6–N1–H1B | 109.5 | C6–C5–C9 | 120.96(19) |
| C6–N1–H1C | 109.5 | C4–C5–C9 | 120.94(19) |
| H1A–N1–H1B | 109.5 | C1–C6–C5 | 122.03(18) |
| H1A–N1–H1C | 109.5 | C1–C2–N1 | 117.73(17) |
| H1B–N1–H1C | 109.5 | C3–C2–N1 | 118.95(16) |
| C1–C2–H2 | 118.6 | C3–C4–H4 | 118.7 |
| C3–C2–H2 | 118.6 | C5–C4–H4 | 118.7 |
| C3–C4–H4 | 119.2 | H1A–N1–H1B | 109.5 |
| C5–C4–H4 | 119.2 | H1A–N1–H1C | 109.5 |
| C1–C8–H8A | 109.5 | H1B–N1–H1C | 109.5 |
| C1–C8–H8B | 109.5 | C1–C6–H6 | 119.0 |
| C1–C8–H8C | 109.5 | C5–C6–H6 | 119.0. |
| C5–C7–H7A | 109.5 | C3–C7–H7A | 109.5 |
| C5–C7–H7B | 109.5 | C3–C7–H7B | 109.5 |
| C5–C7–H7C | 109.5 | C3–C7–H7C | 109.5 |
| C3–C9–H9A | 109.5 | C1–C8–H8A | 109.5 |
| C3–C9–H9B | 109.5 | C1–C8–H8B | 109.5 |
| C3–C9–H9C | 109.5 | C1–C8–H8C | 109.5 |
| H7A–C7–H7B | 109.5 | C5–C9–H9A | 109.5 |
| H7A–C7–H7C | 109.5 | C5–C9–H9B | 109.5 |
| H7B–C7–H7C | 109.5 | C5–C9–H9C | 109.5 |
| H8A–C8–H8B | 109.5 | H7A–C7–H7B | 109.5 |
| H8A–C8–H8C | 109.5 | H7A–C7–H7C | 109.5 |
| H9A–C9–H9B | 109.5 | H7B–C7–H7C | 109.5 |
| H9A–C9–H9C | 109.5 | H8A–C8–H8B | 109.5 |
| H9B–C9–H9C | 109.5 | H8A–C8–H8C | 109.5 |
| | | H8B–C8–H8C | 109.5 |
| | | H9A–C9–H9B | 109.5 |
| | | H9A–C9–H9C | 109.5 |
| | | H9B–C9–H9C | 109.5 |

by using graphite monochromator Mo-Ka radiation ($k$ = 0.71073 Å) at 100 K. The structures were solved by direct methods. Structure solutions, refinement and data output were carried out with SHELX TL programme [15,16]. Hydrogen atoms were placed in geometrically calculated positions by using a rigid model. Images were created with the DIAMOND and MERCURY programme [17,18]. Refinement with anisotropic thermal parameters for non-hydrogen atoms led to $R$ values of 0.0482, 0.0520 respectively for 2,4,6-TMAN and 2,4,6-TMAP. The crystal structures of these salts are shown in Figs. 1 and 4 with thermal ellipsoidal representation at 30% probability level. Crystal parameters, bond lengths and bond angles are shown in Tables 2–4.

### 2.4. Thermal analysis

#### 2.4.1. Non-isothermal TG

Non-isothermal TG of nitrate (30–136 °C) and perchlorate (30–278 °C) salts (wt. 20 mg, 100–200 mesh) were undertaken in a static air at a heating rate of 10 °C/min. using indigenously fabricated TG apparatus [19] fitted with temperature cum controller. The accuracy of the furnace was ±1 °C. A round bottom gold crucible was used as a sample holder. The fraction decomposition ($\alpha$) has been plotted against temperature (°C) and the thermograms are shown in Fig. 7.

#### 2.4.2. Isothermal TG

Isothermal TG studies (wt. 20 mg, 100–200 mesh) of nitrate (80–120 °C) and perchlorate (225–265 °C) were also undertaken in a static air using the above reported TG apparatus at appropriate temperatures. The plots of fractional decomposition ($\alpha$) vs. time (min) are shown in Fig. 8.

Simultaneous TG–DSC analysis on the salts has been done by using DSC instrument at a heating rate of 10 °C/min. (heat flow from 40–700 °C in a nitrogen atmosphere). The TG–DSC thermograms are shown in Fig. 9.

#### 2.4.3. Ignition/explosion delay measurements

The Ignition delay ($\tau_i$) of 2,4,6-TMAN and explosion delay ($\tau_E$) of 2,4,6-TMAP were undertaken, in the temperature range 140–330 °C by taking the sample in an ignition tube (4.5 cm length and 0.4 cm diameter) and the time interval between the insertion of the ignition tube [20] into the TF and the moment of an ignition/explosion noted with the help of a stopwatch, gave the value of ignition delay ($\tau_i$) Similarly moment of an audible explosion gave the value of explosion delay ($\tau_E$). Each run was repeated three times and mean values are reported in Table 5. The $\tau_i$ or $\tau_E$ data were found to fit separately in the equation [21].

$$\log \tau = E/RT + \text{constant} \quad (\tau = \tau_i \text{ for nitrate and } \tau_E \text{ for perchlorate}) \quad (1)$$

where $E$ is the activation energy for thermal ignition/explosion and $T$ the absolute temperature. $E$ assessed by above equation along with the correlation coefficient ($r$) is given in Table 5. Plots of log $\tau$ vs. $1/T$ result in a straight line for both nitrate and perchlorate in accordance with the Eq. (1) as presented in Fig. 10.

**Table 5**
Ignition ($\tau_i$), explosion ($\tau_E$) delay and activation energy ($E$) for 2,4,6-TMAN and 2,4,6-TMAP.

| Compounds | Temperature (°C) | | | | | | $E$ (kJ mol$^{-1}$) | $r$ |
|---|---|---|---|---|---|---|---|---|
| | 125 | 140 | 155 | 170 | 185 | 200 | | |
| 2,4,6-TMAN | DNI | 92 | 78 | 57 | 47 | 36 | 25.77 | 0.9943 |
| Compounds | Temperature (°C) | | | | | | $E$ (kJ mol$^{-1}$) | $r$ |
| | 230 | 250 | 270 | 290 | 310 | 330 | | |
| 2,4,6-TMAP | DNE | 72 | 52 | 35 | 29 | 24 | 36.68 | 0.9922 |

DNI: Did not ignite, DNE: Did not explode, $r$: Correlation coefficient.

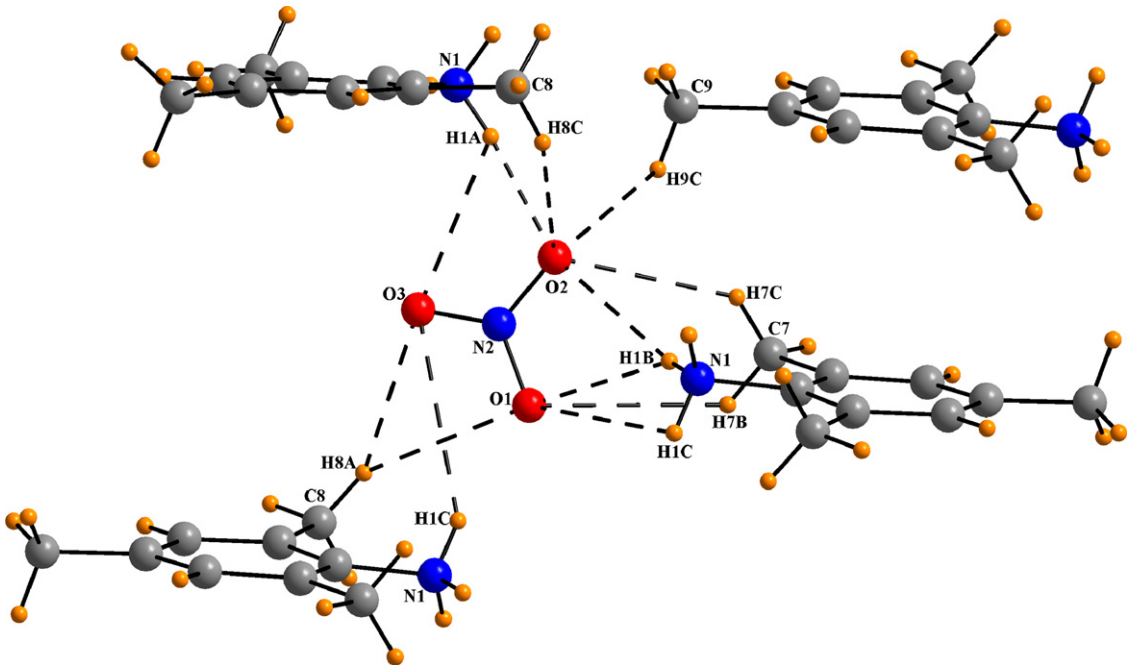


**Fig. 2.** N–H···O and C–H···O intermolecular interactions.

## 3. Kinetics analysis of isothermal TG data

Kinetic analysis of solid state decomposition is usually based on a single step kinetic equation [22]

$$\frac{d\alpha}{dt} = k(T)f(\alpha)$$

where $t$ is the time, $T$ is the temperature, $\alpha$ is the extent of conversion ($0 < \alpha < 1$), $k(T)$ is the rate constant and $f(\alpha)$ is the reaction

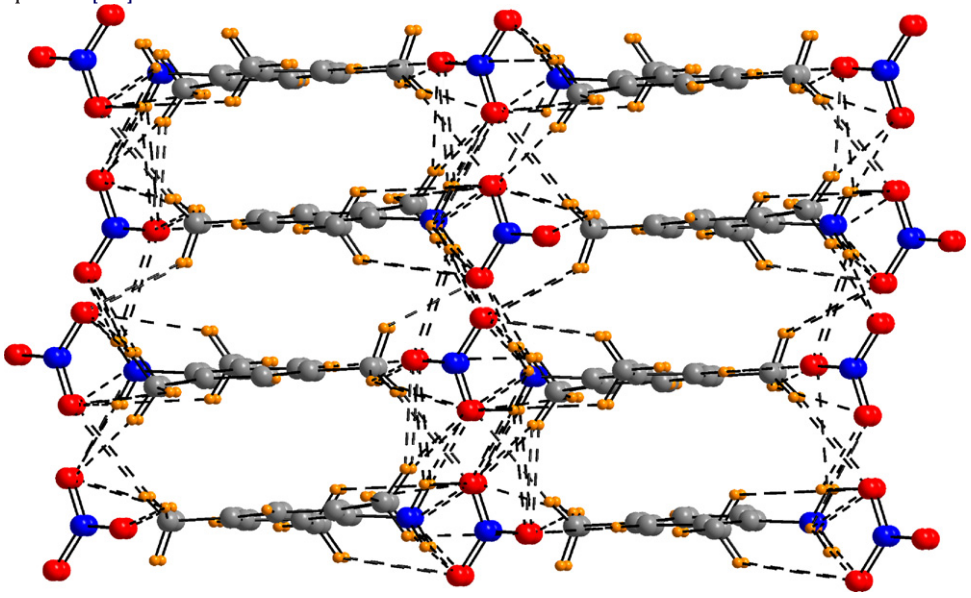

**Fig. 3.** Ladder like packing due to N–H···O and C–H···O interactions (3D view).

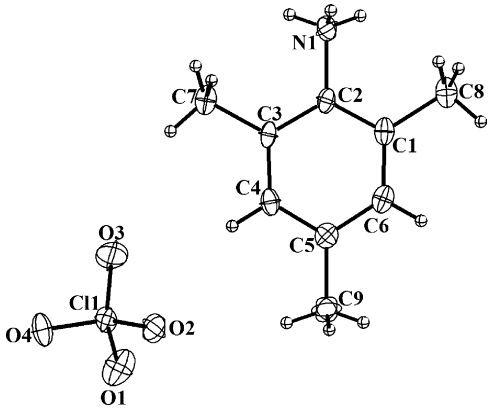


**Fig. 4.** Thermal ellipsoidal presentation for molecular structure of 2 with 30% probability factor.

model, which describes the dependence of the reaction rate on the extent of reactions. The value of $\alpha$ is experimentally derived from the global mass loss in TG experiments. The reaction model may take various forms; The temperature dependence of $k(T)$ can be satisfactorily described by the Arrhenius equation, whose substitution into Eq. (2) yields

$$\frac{d\alpha}{dt} = A \exp\left(-\frac{E}{RT}\right) f(\alpha) \quad (3)$$

where, $A$ is pre exponential factor, $E$ is activation energy and $R$ is the gas constant.

### 3.1. Model fitting method

Rearrangement and integration of Eq. (2) for isothermal conditions gives

$$g_j(\alpha) = k_j(T)t \quad (4)$$

where $g(\alpha) = {}_0\int^{\alpha} [f(\alpha)]^{-1}\, d\alpha$ is the integrated form of the reaction model. The subscript $j$ has been introduced to emphasize that substituting a particular reaction model in Eq. (3) results in evaluating the corresponding rate constant, which is determined from the slope of a plot of $g_j(\alpha)$ vs. $t$. For each reaction model selected, the rate constants are evaluated at several temperatures $T_i$ and Arrhenius parameters (evaluated for isothermal experimental data by the model fitting method) are determined using the Arrhenius Eq. (5) in its logarithmic form

$$\ln k_j(T_i) = \ln A_j - E_j/RT_i \quad (5)$$

### 3.2. Isoconversional method

This method allows the activation energy to be evaluated without making any assumptions about the reaction model. Additionally, the method evaluates the effective activation energy as a function of the extent of conversion which allows one to explore multistep kinetics.

The basic assumption of the isoconversional method [23] is that the reaction model as defined in Eq. (2) is not dependent on temperature or heating rate. Under isothermal conditions, on combining Eqs. (3) and (4) we get-

$$-\ln t_{\alpha,i} = \ln[A_\alpha/g(\alpha)] - E_\alpha/RT_i \quad (6)$$

where $E_\alpha$ is evaluated from the slope of the plot of $-\ln t_{\alpha,i}$ against $T_i^{-1}$. Thus, $E_\alpha$ at various $\alpha_i$ for di-2,4,6-TMAN and di-2,4,6-TMAP have been evaluated and the $E_\alpha$ dependencies are shown in Fig. 11.

## 4. Results and discussions

The molecular structure of 2,4,6-TMAN is shown in Fig. 1 whereas its selected bond distance and bond angles are presented in Tables 3 and 4. The compound crystallizes in the monoclinic space group $P21/n$ ($Z = 4$). The nitrate molecule present in lattice, binds the four molecules of 2,4,6-trimethylaniline (Fig. 2) and responsible for the formation of supramolecule with different types of hydrogen bonding interactions (N–H···O/C–H···O). N–H···O interactions are in the range of 1.989(9)–3.155(2) Å while C–H···O interactions are in the range of 2.521(8)–3.089(15) Å. Due to presence of different interactions, the complex shows a ladder like structure along "*b*" axis in its three dimensional views (Fig. 3) whereas 2,4,6-TMAP crystallizes in triclinic space group $P\text{-}1(Z = 2)$. The molecular structure of complex is shown in Fig. 4. In this com-

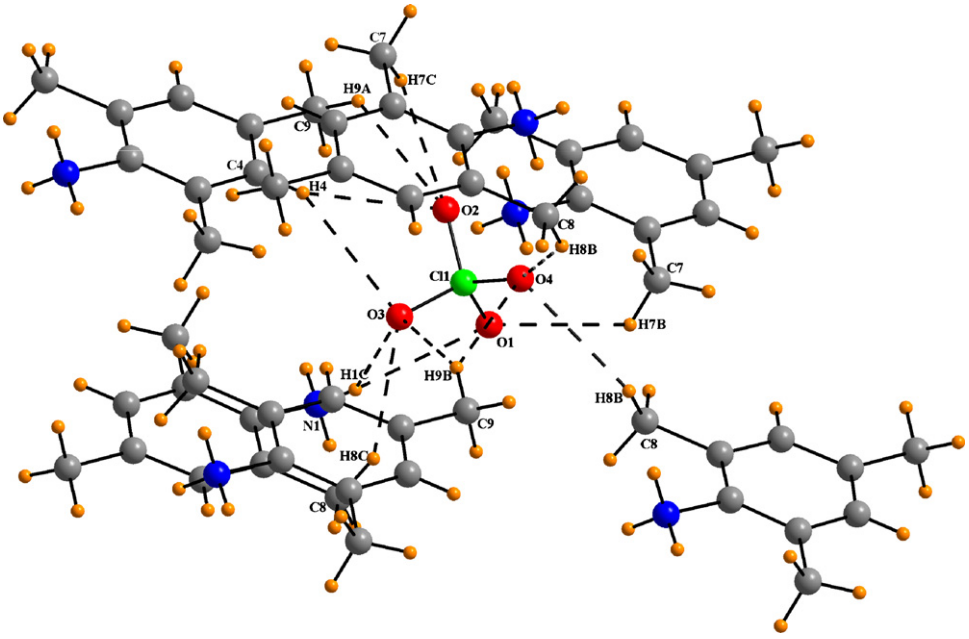


**Fig. 5.** N–H···O and C–H···O intermolecular interactions.

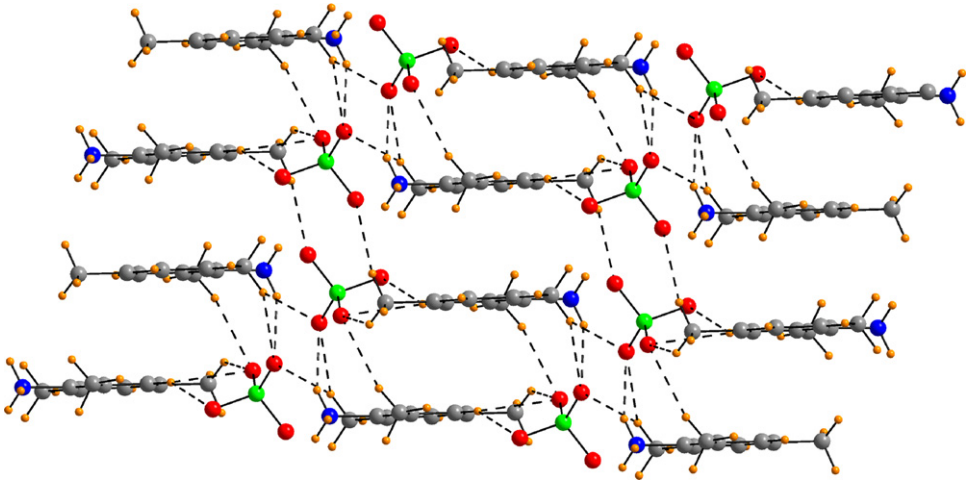

**Fig. 6.** Ladder like packing due to N–H···O and C–H···O interactions (2D view).

plex, one perchlorate ion binds the six molecules of amine through N–H···O/C–H···O type of hydrogen bonding (Fig. 5). The N–H···O interactions are in the range of 2.158–2.703 Å while C–H···O interactions are in the range of 2.616(17)–3.000(7) Å. These interactions also resulted the formation of a ladder like structure along "*b*" axis (Fig. 6).

TGA (Fig. 7) undertaken in static air tells beyond doubt that both nitrate and perchlorate underwent ignition and explosion, respectively, leaving the black residue. Further TG–DSC ($N_2$ atmosphere) of 2,4,6-TMAN also inferres that the sample also undergo internal oxidation–reduction reaction leading to ignition. It is stated that due to high explosive sensitivity, TG–DSC of 2,4,6-TMAP could not be undertaken (Figs. 8–10).

The kinetics of the thermal decomposition of both salts were evaluated using 14 mechanism-based kinetics models [9] by choosing a "best fit" model based on the value of the correlation coefficient *r* close to 1. Among various values of r (obtained from different models) the highest value of r correspond to model 13 and 5 respectively for 2,4,6-TMAN and 2,4,6-TMAP. Based on these observations; the rate controlling process in the decomposition of 2,4,6-TMAN salt is chain growth of nuclei whereas for 2,4,6-TMAP, it is one dimensional diffusion. Nevertheless, our calculation shows that for 2,4,6-TMAN $E_a$ obtained from different models have nearly same values irrespective to the equation used. Though values of $E_a$ are different for 2,4,6-TMAP. Average value of activation energy (from isothermal TG data (Table 6) were found to be 77.9 and 118.2 kJ mol$^{-1}$ respectively for 2,4,6-TMAN and 2,4,6-TMAP. The isoconversional method is known to permit estimation of activation energy independent of the model used. This method is being used to establish a relation between activation energy and extent of conversion ($\alpha$) of the sample. As it is clear from Fig. 11 that for a particular sample, activation energy has different value at a different $\alpha$. Further to evaluate the sensitivity of nitrate and perchlorate salts, there ignition and explosion delay measurement were carried out; Although both are stable at room temperature but they ignite/explode when subjected to sudden high temperature range (140–200 °C for 2,4,6-TMAN and 250–330 °C for 2,4,6-TMAP). Their $\tau_i$ and $\tau_E$ as reported in Table 5. The energy of activation for ignition/explosion ($E$) are 25.77 and 36.68 kJ mol$^{-1}$ for 2,4,6-TMAN and 2,4,6-TMAP respectively.

The activation energy calculated by isothermal TG and ignition/explosion delay measurement has different values which may

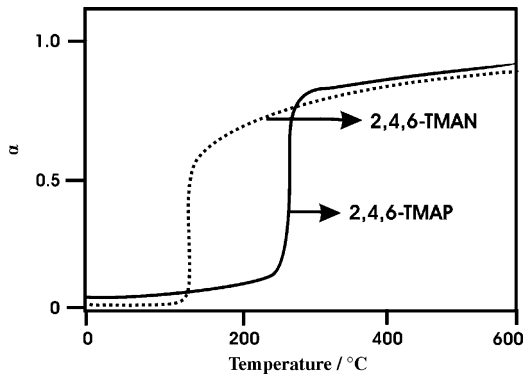


**Fig. 7.** Non-isothermal TG of 2,4,6-TMAN and 2,4,6-TMAP under static atmosphere.

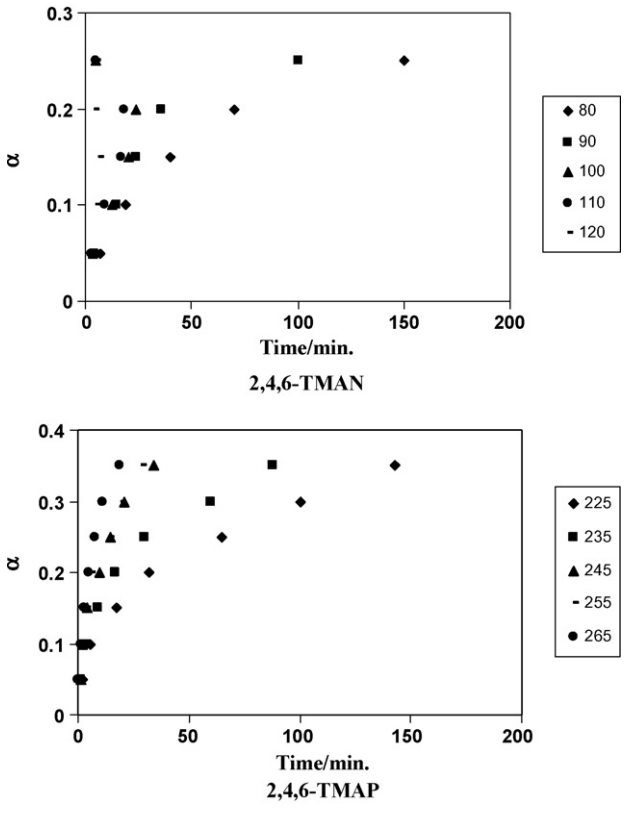


**Fig. 8.** Isothermal TG of 2,4,6-TMAN and 2,4,6-TMAP.

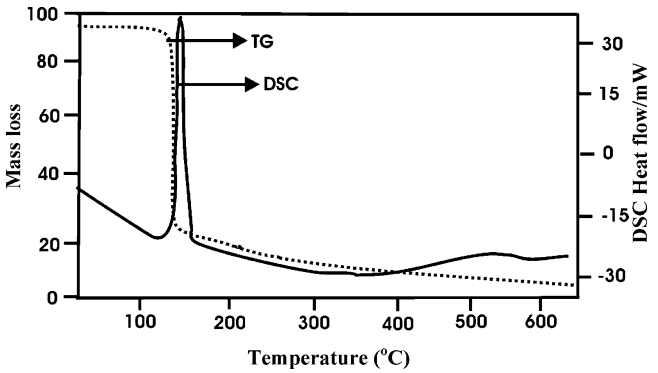


**Fig. 9.** Simultaneous TG–DSC curves of 2,4,6-TMAN in $N_2$ atmosphere.

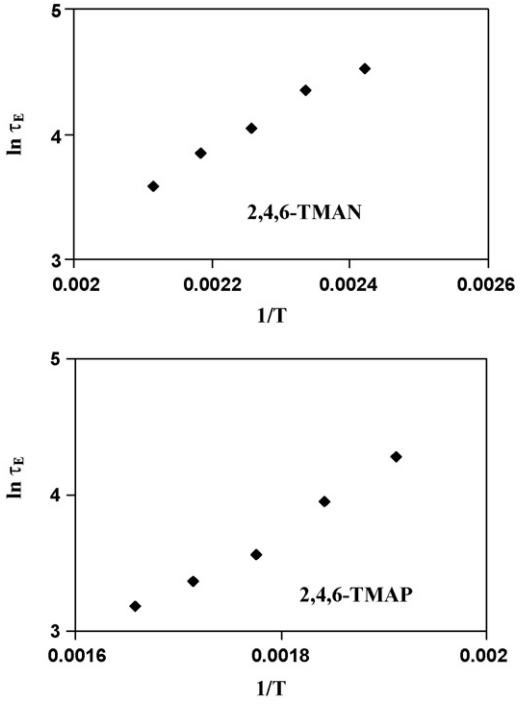


**Fig. 10.** Graph of ln $D_i$ vs. $1/T$ (2,4, 6-TMAN) and ln $D_E$ vs. $1/T$ (2,4,6-TMAP).

**Table 6**
Arrhenius parameters for the isothermal decomposition of 2,4,6-TMAN and 2,4,6TMAP.

| | 2,4,6-TMAN | | 2,4,6-TMAP | |
|---|---|---|---|---|
| Reaction Models | $E_a$ (kJ mol$^{-1}$) | $r$ | $E_a$ (kJ mol$^{-1}$) | $r$ |
| Power law | 76.6 | 0.9809 | 118.4 | 0.9727 |
| Power law | 75.6 | 0.9806 | 118.4 | 0.9727 |
| Power law | 73.4 | 0.9800 | 118.3 | 0.9728 |
| Power law | 58.9 | 0.9721 | 118.2 | 0.9734 |
| One-dimensional diffusion | 51.2 | 0.9623 | 118.2 | 0.9738 |
| Mampel (first order) | 64.1 | 0.9761 | 118.2 | 0.9733 |
| Avrami-Erofeev | 51.9 | 0.9679 | 117.8 | 0.9727 |
| Avrami-Erofeev | 74.2 | 0.9803 | 118.3 | 0.9728 |
| Avrami-Erofeev | 71.8 | 0.9796 | 118.3 | 0.9729 |
| Contracting sphere | 64.9 | 0.9766 | 118.2 | 0.9733 |
| Three-dimensional diffusion | 48.5 | 0.9577 | 118.3 | 0.9590 |
| Contracting cylinder | 65.3 | 0.9767 | 118.2 | 0.9732 |
| Prout-Tomkins | 77.9 | 0.9812 | 118.5 | 0.9727 |
| Ginstling-Brounshtein | 49.2 | 0.9593 | 96.1 | 0.9527 |

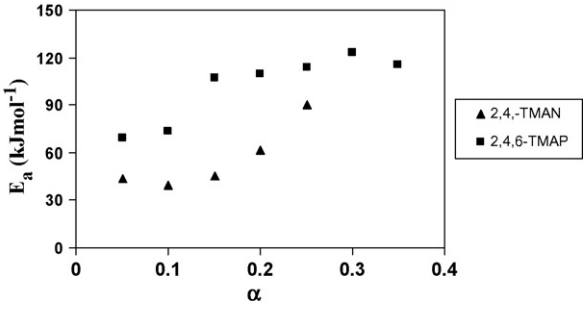


**Fig. 11.** Dependence of the activation energy ($E_a$) on the extent of conversion ($\alpha$).

be due to the different temperature ranges. Regarding, X-ray crystallography of nitrate one $NO_3^-$ ion is attached with four moiety of 2,4,6-trimethylaniline through hydrogen bonding, whereas in perchlorate salt one $ClO_4^-$ ion is bonded with six moiety of amine. Since the number of hydrogen bonds in case of perchlorate salts is higher than the nitrate salt, hence activation energy value for perchlorate salts was found to be higher. From Scheme 2, it is clear beyond doubt that at a higher temperature (nitrate and perchlorate) salts in solid phase undergo weakening of N–H bond to facilitate proton transfer from – $NH_3^+$ to $NO_3^-$ and $ClO_4^-$ to form H···O bond in condensed phase. Oxidation–reduction reaction between fuel (amine part) and oxidizer (nitric acid and perchloric acid) leads to decomposition followed by ignition or explosion to form finally gaseous product leaving a black carbon residue. Further

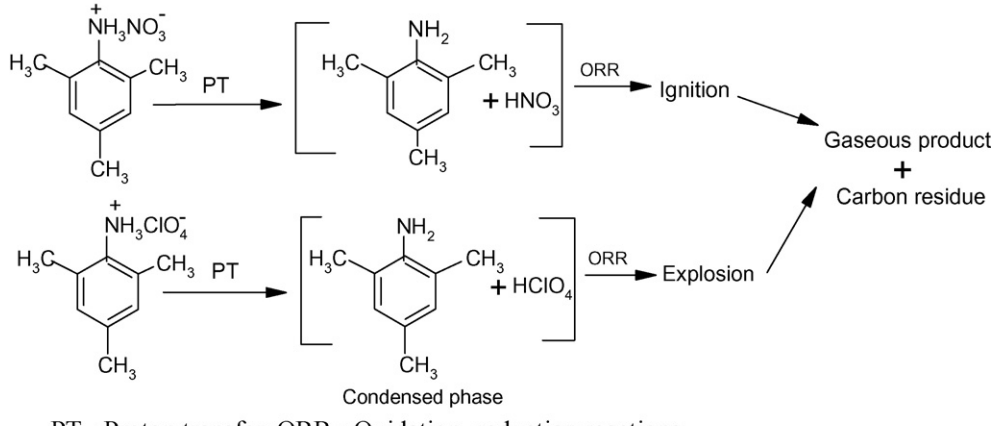


**Scheme 2.** Thermal decomposition of 2,4,6-TMAN and 2,4,6-TMAP salt. PT = Proton transfer, ORR = Oxidation–reduction reactions.

the O/H ratio of both 2,4,6-TMAN and 2,4,6-TMAP salts is less than 1. Hence $NH_3$ may be a decomposition product. Brill and Oyumi and Nambiar et al. [24,25] have also reported $NH_3$ as a decomposition product of methylammonium nitrate and perchlorate. In thermolysis of 2,4,6-TMAP some of the perchloric acid may be consumed by reaction with $NH_3$ to produce intermediate $NH_4ClO_4$ (not identified). Combination of $NH_3$ with $HNO_3$ to form intermediate $NH_4NO_3$ has been reported in the thermolysis of pentaerythrityltetra ammonium nitrate and 1,2,3-triaminoguanidinium nitrate [26]. It is also evident that a part of each salt have also undergone sublimation, which was confirmed by heating each salt separately at an appropriate temperature.

## 5. Conclusion

Nitrate and perchlorate salts of 2,4,6-trimethyl aniline undergo decomposition followed by, respectively, ignition and explosion. Proton transfer from $-NH_3^+$ to $NO_3^-$ and $ClO_4^-$ is primary step to form amine and corresponding acids ($HNO_3$ and $HClO_4$) in condensed phase where oxidation–reduction yields gaseous products. The activation energy of 2,4,6-TMAN and 2,4,6-TMAP were found to be 77.9 and 118.2 kJ $mol^{-1}$ respectively.

## Acknowledgements

Thanks are due to Head, Department of Chemistry DDU Gorakhpur University for providing laboratory facilities. SAIF, Cochin for TG–DSC data. Authors are also thankful to UGC for financial assistance to Manisha Kapoor and CSIR for Emeritus Scientist to Dr. G. Singh.

## Appendix A. Supplementary data

Supplementary data associated with this article can be found, in the online version, at doi:10.1016/j.jhazmat.2009.08.058.

## References

[1] G. Singh, C.P. Singh, P. Felix, Recent Researches on Thermolysis of Energetic Materials, Nova Publication Inc, New York, 2008.
[2] G. Singh, D.K. Pandey, Studies on energetic compounds part 30: kinetics and mechanism of thermolysis of bis (diethylenetriamine) metal (II) nitrate complexes, J. Therm. Anal. Calorim. 76 (2004) 507–519.
[3] J.T. Kummer, Thermal decomposition of ammonium nitrate, J. Am. Chem. Soc. 69 (1947) 2559–2562.
[4] G. Singh, I.P.S. Kapoor, M. Mannan, J. Kaur, Studies on energetic compounds, part 7; kinetic of salts of $HNO_3$ and $HClO_4$ a review, J. Hazard. Mater. A 79 (2000) 1–18.
[5] R. Chem, T.P. Russell, A.L. Rheingold, T.B. Brill, Thermal decomposition of energetic materials, 44. Rapid thermal decomposition of the propyl-1,3-diammonium salts of $NO_3^-$ and $ClO_4^-$, and the crystal structure of the $ClO_4^-$ salt, J. Cryst. Spect. Res. 21 (1991) 167–171.
[6] L. Erdey, S. Gal, Thermoanalytical investigations of high temperature fusion reactions, Talanta 10 (1963) 23–36.
[7] L. Erdey, S. Gal, G. Liptay, Thermoanalytical properties of analytical grade reagents: ammonium salts, Talanta 11 (1964) 913–940.
[8] I.P.S. Kapoor, P. Srivastava, G. Singh, Preparation, characterization & thermolysis of phenylenediammonium dinitrate salts, J Hazard. Mater. 150 (2008) 687–694.
[9] I.P.S. Kapoor, P. Srivastava, G. Singh, U.P. Singh, R. Fröhlich, Preparation, crystal structure and thermolysis of diperchlorate salts, J. Phys. Chem. A 112 (4) (2008) 652–659.
[10] G. Singh, I.P.S. Kapoor, S. Jacob, Studies on energetic compounds- Part 19: Preparation and thermolysis of *N*-Methylanilinium and *N,N*- dimethylanilinium nitrate and perchlorates, J. Sci. Ind. Res. 59 (2000) 575–582.
[11] G. Singh, B.P. Baranwal, I.P.S. Kapoor, D. Kumar, C.P. Singh, R. Fröhlich, Preparation, X-ray crystallography, and thermal decomposition of some transition metal nitrate complexes with hexamethylenetetramine, J. Therm. Anal. Calorim. 91 (2008) 971–976.
[12] G. Singh, B.P. Baranwal, I.P.S. Kapoor, D. Kumar, R. Fröhlich, Preparation, X-ray crystallography and thermal decomposition of some transition metal perchlorate complexes of hexamethylenetetramine, J. Phys. Chem. A 111 (2007) 12972–12976.
[13] G. Singh, D.K. Pandey, Studies on energetic compounds, Part 40: kinetics of thermal decomposition of bis (propylenediamine) metal perchlorate complexes, J. Therm. Anal. Calorim. 82 (2005) 253–260.
[14] G. Singh, I.P.S. Kapoor, J. Singh, J. Kaur, Role of proton transfer reaction in the thermolysis of alkyl and arylammonium salts, Ind. J. Chem. 39 B (2000) 1–9.
[15] G.M. Sheldric, Phase annealing in SHELX-90: direct methods for larger structures, Acta Crystallogr. A 46 (1990) 467–473.
[16] G.M. Sheldric, SHELXTL- NT, Version 6.12, Reference Manual, University of Gottingen, Germany, 2000.
[17] B. Klaus, DIAMOND, Version 1.2 c, University of Bonn, Bonn, Germany, 1999.
[18] F.H. Allen, The Cambridge structural database: a quarter of a million crystal structures and rising, Acta Crystallogr. B 58 (2000) 380–388.
[19] G. Singh, R.R. Singh, Indigenously fabricated apparatus for thermogravimetric analysis, Res. Ind. 23 (1978) 92–93.
[20] E.S. Freeman, S. Gorden, The application of the absolute rate theory of the nitrate- magnesium, sodium nitrate- magnesium, J. Phys. Chem. 60 (1956) 867–871.
[21] H. Henkins, R. McGill, Rates of explosive decomposition of explosives experimental and theoretical kinetics study as a function of temperature, Ind. Eng. Chem. 44 (1952) 1391–1394.
[22] M.E. Brown, D. Dollimore, A.K. Galaway, Reactions in the Solid State, in: Comprehensive Chemical Kinetics, 22, Elsevier, Amsterdam, The Netherlands, 1960, pp.1–340.
[23] S. Vyazokin, I. Dranca, X. Fan, R. Advincula, Kinetics of the thermal and thermo-oxidative degradation of polystyrene-clay nanocomposite, Macromol. Rapid Commun. 25 (2005) 498–503.
[24] Y. Oyumi, T.B. Brill, Thermal decomposition of energetic materials, 25: shifting of the dominant decomposition site by backbone substitution of alkylammonium nitrate salts, J. Phys. Chem. 91 (1987) 3657–3661.
[25] P.R. Nambiar, V.P. Vernekar Pai, R.S. Jain, Thermal decomposition of methyl ammonium perchlorate, J. Therm. Anal. 7 (1975) 587–592.
[26] T.P. Russell, T.B. Brill, Thermal decomposition of energetic materials. 39. Fast thermolysis patterns of poly (methyl), poly (ethyl), and primary alkylammonium mononitrate salts, Propellant Explos. Pyrotech. 1 (1990) 66–72.